Single-particle diffusion in dense inhomogeneous colloid suspensions in ribbon channels

Emily Wonder, Binhua Lin, and Stuart A. Rice

Single Particle Diffusion in Dense Inhomogeneous Colloid Suspensions in Ribbon Channels

Emily Wonder, Binhua Lin* and Stuart A. Rice*

[1]Department of Chemistry, CARS and The James Franck Institute, The University of Chicago, Chicago, IL 60637

Abstract

We report the results of a study of single particle diffusion in dense colloid fluids confined in a ribbon channel geometry that is intermediate between quasi-one-dimensional (q1D) and quasi-two-dimensional (q2D). This study complements a previous study of pair diffusion in the same system [Phys. Rev. E **82**, 031403 (2010)]. In all of the systems studied the colloid density distribution transverse to the ribbon channel is stratified with peak amplitudes that depend on the colloid density. Although the virtual walls that confine a stratum are structured with a scale length of the colloid diameter, that structure does not have an apparent influence on the single particle diffusion, which shows the characteristic features of diffusion in a q1D channel with smooth walls. We find that for all channel widths and packing fractions studied the single particle transverse diffusion coefficient in a stratum is smaller than the single particle longitudinal diffusion coefficient in the same stratum, and that the single particle longitudinal diffusion coefficient varies very little from stratum to stratum, being only slightly smaller in the dense strata next to the walls than in central strata. The lack of variation of the longitudinal

diffusion coefficient with apparent stratum density is explained by application of the Fischer-Methfessel approximation to the local density in an inhomogeneous liquid. The ratio of the transverse to longitudinal diffusion coefficients varies very slowly with ribbon width, implying a very slow transition from q1D to q2D behavior.

* Corresponding authors: Binhua Lin blin@uchicago.edu and Stuart A. Rice
sarice@uchicago.edu

I. Introduction

Interest in the effects of confinement on the particle dynamics and the hydrodynamic interactions in dense colloid fluids has attracted considerable attention in the last decade, driven in part by fundamental questions concerning the influence of dimensionality on the transport properties of a system and in part by the practical applications of confined colloid suspensions [1-3]. A survey of the relationships between structure, confinement and particle-particle interaction can be found in Ref. [4].

We recently reported studies of the density distribution and the transverse and longitudinal pair-diffusion coefficients in colloid suspensions confined in ribbon channels whose width varies from about 2 to 12 colloid diameters, a geometry that is intermediate between q1D and q2D [5, 6]. The main structural feature of such a system is that the density distribution of the fluid transverse to the to the ribbon walls is stratified, which has also been observed in three-dimensional colloid suspensions near a wall or narrowly confined between two smooth walls [7-9]. We consider a system to have q1D character if the channel that confines it is less than two particle diameters wide, and to have q2D character if it is confined between two smooth walls separated by less than two particle diameters. In the q1D system the mean positions of the centers of the colloid particle lie on a line, but small displacements perpendicular to the line occur. In the q2D system the mean positions of the centers of the colloid particle lie in a plane, but small displacements perpendicular to the plane occur. In both the q1D and q2D systems one particle cannot pass another via motion perpendicular to the line or plane of centers.

The focus of our previous studies was on the transition between q1D and q2D behavior in dense colloid suspensions, using the ribbon channels as a vehicle. We found that the order along

the strata is characteristic of a q1D liquid, even at a density near to close packing [6]. However, if the stratified density distribution is ignored the order on the length-scale of the width of the channel is characteristic of a q2D liquid or solid, supporting the view that ribbon suspensions fall into the unknown domain between q1D and q2D geometries. The dynamics of the colloid motion in the ribbon systems, examined with pair-diffusion coefficients (that is, via the influence of hydrodynamic couplings between a pair of colloid particles), are found to be multifaceted [5]. While the hydrodynamic coupling exhibits q2D characteristics already for relatively narrow channels when measured along the channels axis, it continues to deviate from the expected q2D behavior even for the widest channels studied when it is measured transverse to the channel axis. Furthermore, colloids within each stratum behave as if they are confined in q1D geometry.

In this short paper we again examine the transition between q1D and q2D behavior in colloid suspensions confined in ribbon channels, focusing attention on the one-particle diffusion coefficient. Our motivation for doing so is contained in three questions relevant to the q1D to q2D transition that are not addressed by our previous study. First, given the stratification of the density distribution transverse to the ribbon channel, does the corrugation of the nearest neighboring strata affect the short-time single-particle diffusion coefficient? Second, does the short-time single-particle diffusion coefficient vary from stratum to stratum across the channel, and/or from peak to trough of the density distribution? Third, if the stratification of the transverse density distribution in the ribbon channel is disregarded, by averaging over all the strata in the channel, how does the single particle diffusion coefficient for the confined suspension differ from that in an infinite q2D suspension?

II. Experimental Details

Detailed sample preparation and data processing procedures have been described in our previous report on the equilibrium structure and pair-diffusion in the same colloid suspensions and ribbon channels[5, 6]. Briefly, our experimental system consists of a sample cell that contains a single layer of a silica spherical colloid suspension (Duke Scientific, $\sigma = 1.58 \pm 0.04$ μm, density $2.2\,g/cm^3$) confined to long narrow channels of various widths, w, but the same depth h ($h=3$ μm). The channels were printed on a polydimethysiloxane (PDMS) substrate from a master pattern fabricated lithographically (Stanford Nanofabrication Facility). A diagram of the experimental arrangement and images of the colloids in the ribbon channels are displayed in Figure 1. Digital video microscopy was used to extract time-dependent two-dimensional trajectories of the colloid particles (with time resolution 0.033 s), and the short-time domain within which the in-stratum diffusion coefficient was obtained was $0.033 < t < 0.2 s$.

The data for the ribbon channels are compared with those for the q1D and q2D geometries, which were obtained using the same colloid preparation. In the case of the q1D geometry, at each density a single file of the same silica spheres was confined in a channel whose width and depth were 3 μm [10]; in the case of the q2D geometry, at each density a single layer of the same silica spheres was confined between two hard walls whose gap was 1.7 μm [11].

We note that the ribbon channels are unconfined at the top. Nevertheless, the microscope images show that the colloid particle centers lie in the focal plane and remain there for the duration of the experiments. We rarely observe jumping of particles out of or into the ribbon channel. Furthermore, as shown in earlier studies of colloid suspensions in q1D channels that are unconfined at the top [10], the influence of hydrodynamic interactions is well accounted for

when the channel is represented as a fully closed capillary with effective radius very close to the channel width (and depth). Put another way, because the fluid in the q1D channel and above are quiescent, there must be a boundary in the fluid that contacts the lips of the channel and on which the fluid velocity vanishes. We assume that the same situation exists for the ribbon channels.

The particle density distributions in all samples in the ribbon channels were uniform along the x-axis (the direction of the channel). However, the extent of particle displacement transverse to the channel (y-direction) is less than the width of the channel. We attribute this to the non-wetting property of the PDMS wall. The effective width of the channel, w_{eff}, is approximately 1 μm less than w along each wall, as calculated from the histogram of the colloid particle positions and the distance between the most widely separated density peaks. We assume, likewise, that the effective depth of all the channels is $h_{eff} \approx 2 \mu$m. For clarity, the experimental data sets will be referred to using the fabricated channel width w. The packing fraction was calculated using $\phi = N\pi\sigma^2 / 4lw_{eff}$ with l the length of the channel in the field of view (108 μm), and N the average number of particles in the viewed section of the channel. The transverse density distribution in the ribbon channel was separated into strata centered on the peaks with widths defined by the minima in the distribution. The single particle diffusion coefficient along (longitudinal) and perpendicular (transverse) to each stratum was calculated from the variation of the mean square displacement with time. The values reported for the diffusion coefficients refer to the short time linear regime wherein the mean square displacement is proportional to time.

III. Results and Discussion

We first address questions 1 and 2 from Section I using the experimental results shown in Figures 2-4.

We display in Figure 2 samples of the in-stratum short-time single-particle diffusion coefficients for ribbon channels with widths of 5 μm (Fig. 2A), 8 μm (Fig. 2B), 11 μm (Fig. 2C), 14 μm (Fig. 2D), and 20 μm (Fig. 2E), all with packing fraction $\phi \approx 0.4$. The figure shows a superposition of the transverse density profile in the ribbon channel, *P(y)*, and the short time single particle diffusion coefficients along and perpendicular to the strata of the transverse density distribution. The diffusion coefficient data, also listed in Table 1, are for the strata in the density profile shown by the symbols. The dominant qualitative features of the data, for all packing fractions, are the following:

1. For all channel widths and packing fractions studied the single particle transverse diffusion coefficient in a stratum is smaller than the single particle longitudinal diffusion coefficient in the same stratum.

2. The single particle longitudinal diffusion coefficient varies very little from stratum to stratum, being only slightly smaller in the dense strata next to the walls than in central strata. The single particle transverse diffusion coefficient is much smaller in the dense strata next to the walls than in central strata, but varies little in the central strata.

3. For the widest channel and highest density studied (20 μm channel with packing fraction $\phi \approx 0.41$), the transverse density distribution has very distinct peaks near the walls and is nearly uniform in the central region. We subdivide this transverse density distribution into equal width strata centered on the maxima and minima of the distribution, and determine the corresponding diffusion coefficients. As shown in Fig. 3, both the single

7

particle longitudinal and transverse diffusion coefficients are sensibly the same for strata centered on minima and maxima of the density distribution, except for the strata closest to the walls of the channel.

4. There is a small variation across the inner strata of the density distribution of the ratio of the single particle transverse to longitudinal diffusion coefficients. That ratio is larger for the central stratum than for the surrounding strata. The difference is only of the order of 2-5%, but consistent for all channels.

5. At the largest packing fraction studied, $\phi \approx 0.42$, as the ribbon width is increased there is a weak increase of the central stratum value of the ratio of the single particle transverse to longitudinal diffusion coefficients.

As reported previously, in a q1D colloid suspension the hydrodynamic interaction between particles decays exponentially with scale length w, and two body hydrodynamic interactions remain dominant up to high particle density [10]. In a q2D colloid suspension confined between two hard walls with a small separation $H \sim \sigma$, the far field flow induced by the motion of a colloid particle has a momentum monopole contribution that is cut off by the boundary conditions at distances larger than the confinement width H, and a mass dipole contribution that decays as $(H/r)^2$, with the anisotropy of the dipolar flow field responsible for the negative sign of the coupling that affects the transverse pair diffusion coefficient [11].

Observation 1 clearly implies that the single particle diffusion coefficient in the ribbon channel retains at least some q1D characteristic behavior in all of the systems studied, and observations 4 and 5 imply that the approach to q2D behavior is slow but noticeable. A sampling of the particle trajectories, such as shown in Fig. 4, reveals that there are very few exchanges of particles between strata even when the instantaneous particle displacements

transverse to the average stratum midline are substantial. We note that the trajectories shown in Fig. 4 are 5 s long, much longer than the time interval, 0.18 s, used to calculate the short time diffusion coefficients we report. Figure 4 shows that on the time scale of interest the strata deform and remain distinct, thereby restricting the magnitude of the transverse particle displacement relative to the longitudinal particle displacement.

This paper has focused attention on the transition from q1D to q2D behavior in dense colloid suspensions, wherein both excluded volume and hydrodynamic interaction effects are important. In a dense suspension, because of the complex fluid flows generated by interaction between the boundary conditions imposed by both the walls and any instantaneous configuration of impenetrable particles, parsing these contributions is difficult. In contrast, the influence of a nearby wall on the hydrodynamic interaction with an otherwise isolated spherical particle is well understood. Theoretical and experimental studies [12, 13] (and references therein) show that both the diffusion coefficients of an isolated particle perpendicular to a wall and parallel to a wall are reduced relative to that in the bulk liquid. At a distance from one wall of one particle radius the perpendicular diffusion coefficient is reduced to zero and the parallel diffusion coefficient is reduced to less than 0.4 of the value in the bulk liquid. The diffusion coefficients return to 0.8 of the bulk value only at distances from the wall of about 6 and 3 particle radii, respectively. The effect on isolated particle diffusion of several walls is tolerably accounted for by a linear superposition of the effects of each wall [13]. It is clear, from observations 2 and 3, that our data do not follow the theoretical predictions for the wall-drag effect on isolated particles.

A full theoretical analysis of the influence of the density of the suspension on the single particle diffusion coefficients parallel and perpendicular to a wall is not available. However, it is reasonable to expect that the complex fluid flows needed to satisfy the zero slip boundary

condition on the surfaces of all particles in the system will severely alter the particle motion. A qualitative description of how the presence of other particles in a dense colloid suspension influences the dependence of the one-particle diffusion coefficient on separation from a wall has been provided by Brady and coworkers [8]. Assuming that particle-wall and particle-particle near field hydrodynamic interactions are the same because they have the same singular behavior near contact, in a high-density suspension a particle cannot distinguish between a near neighbor particle and the wall, thereby greatly reducing the dependence of the one-particle diffusion coefficient on separation from the wall. Indeed, evanescent light scattering studies of colloid particle motion near a wall in a three-dimensional system [7, 8] show that as the concentration of colloid particles increases the effect of the wall on the diffusion coefficient decreases. And a confocal microscopy study of a dense q2D colloid suspension between hard walls [9] finds that the diffusion coefficient for motion parallel to the wall is sensibly independent of distance from the wall.

In the experiments reported in this paper a colloid particle is always very close to one wall (the floor of the cell) and to many other particles, and the sidewall heights are only about two particle diameters. Extrapolating the observations relevant to 3D systems to the ribbon channel experiments, we expect that if there is one particle in the ribbon channel only motion parallel to the floor of the channel is possible, and that if the zero slip and impenetrability boundary conditions at the sidewalls are dominant despite the limited wall height, the expected transverse and longitudinal diffusion coefficient of an isolated colloid particle in a ribbon channel will vary strongly across the channel, unlike what we observe for a dense suspension in a ribbon channel. The qualitative argument offered by Brady is equally applicable to colloid motion in three dimensions near a wall and to colloid motion in a ribbon channel. We conclude

that excluded volume and the associated structural and lubrication effects grossly alter the hydrodynamic interactions and render the one-particle diffusion coefficient sensibly independent of particle-wall separation.

It is arguable that observation 3 is the least expected of the results, since the strata show substantial differences of their local densities as the ribbon width and colloid concentration are changed. In a bulk suspension the diffusion coefficient is a strong function of the colloid density, and a conventional local density representation of the properties of the stratified suspension in the ribbon channel leads to the expectation of a corresponding variation with stratum density of the diffusion coefficient. We interpret observation 3 using the Fischer-Methfessel representation of the local density in an inhomogeneous fluid. Fischer and Methfessel pointed out that to sustain a density gradient in an inhomogeneous liquid there must be a balancing force that is not captured by representing the local density as a point function [14]. They showed that to lowest order the source of the force is, typically, interaction with nearest neighbors of a molecule, and therefore defined the local density as an average over a volume with radius one particle diameter. It has been shown that this approximation provides a good description of the pair correlation function in the inhomogeneous transition region in the liquid-vapor interface [15]. The application to our results follows from the observation that at the colloid suspension densities we have studied the hydrodynamic interactions between colloid particles in q1D and q2D geometries are determined by the pair correlation function. Applying the Fischer-Methfessel approximation to the description of our system implies defining the local density by averaging over neighboring strata, thereby sensibly removing the density variation of the pair correlation function and, thereby, the density variation of the friction coefficient.

Finally, we address question 3 raised in Section I. We display in Fig. 5 the mean square

displacement of a particle as a function of time for colloid suspensions with $\phi \approx 0.27$ in a q1D channel, ribbon channels with widths 5 μm – 20 μm, and a q2D geometry. These mean squared displacements were calculated for all particles across the full width of the ribbon channel. In all of these systems the mean square displacement increases linearly with time for short time, but only for the q2D geometry is it linear at long time. The data for the q1D channel clearly show a deviation of the mean square displacement from a linear dependence on time and an approach to the predicted dependence on the square root of time. The mean square displacement data for the 5 μm – 20 μm channels show deviations from a linear dependence on time that are similar to that observed in q1D, but decreasing as the channel width increases. Note that the long time dependence of the mean square displacement for a particle in the widest ribbon channel still deviates from the q2D linear time dependence. The effect of the confinement is clearly shown as the width of the channel is reduced.

V. Conclusion

We have examined the behavior of single particle short-time diffusion in a dense colloid fluid confined in a ribbon channel in which the transverse density distribution is stratified. By addressing the questions raised in the Introduction, we see again that this stratified dense liquid exhibits characteristics of both q1D and q2D fluids, depending on the length-scale over which the properties are probed. This conclusion confirms that reached in our previous studies of the equilibrium structural properties, via measurements of the pair-correlation functions, and hydrodynamic coupling, via measurements of the pair-diffusion coefficients, of the same colloid particles in the same ribbon channels. The most striking result of this work is that, when measured along individual strata peaks or valleys, the longitudinal diffusion coefficients are essentially uniform across the width of the channel, whereas the transverse diffusion coefficients

are sensitive to the variation of the density distribution and the wall-drag effect, as observed in a dilute bulk colloid fluid. The findings in this study and our previous reports should provide useful insights into the phenomena observed on different length scales in biological structures and/or micro-fluidic applications that are intermediate between q1D and q2D.

VI. Acknowledgements

VI. References

[1]   C. Bechinger, Curr. Opin. Colloid In. **7**, 204 (2002).
[2]   H. Diamant, J. Phys. Soc. Jpn. **78**, 041002 (2009).
[3]   T. M. Squires and S. R. Quake, Rev. Mod. Phys. **77**, 977 (2005).
[4]   S. A. Rice, Chem. Phys. Lett. **479**, 1 (2009).
[5]   S. Novikov, S. A. Rice, B. Cui, H. Diamant, and B. Lin, Phys. Rev. E **82**, 031403 (2010).
[6]   T. R. Stratton, S. Novikov, R. Qato, S. Villarreal, B. Cui, S. A. Rice, and B. Lin, Phys. Rev. E **79**, 031406 (2009).
[7]   P. Holmqvist, J. K. G. Dhont, and P. R. Lang, Phys. Rev. E **74**, 021402 (2006).
[8]   V. N. Michailidou, G. Petekidis, J. W. Swan, and J. F. Brady, Phys. Rev. Lett. **102**, 068302 (2009).
[9]   C. R. Nugent, K. V. Edmond, H. N. Patel, and E. R. Weeks, Phys. Rev. Lett. **99**, 025702 (2007).
[10]   B. Cui, H. Diamant, and B. Lin, Phys. Rev. Lett. **89**, 188302 (2002).
[11]   B. Cui, H. Diamant, B. Lin, and S. A. Rice, Phys. Rev. Lett. **92**, 258301 (2004).
[12]   J. Happel and H. Brenner, *Low Reynolds Number Hydrodynamics* (Kluwer Academic Publishers Group, Dordrecht, 1983).
[13]   B. Lin, J. Yu, and S. A. Rice, Phys. Rev. E **62**, 3909 (2000).
[14]   J. Fischer and M. Methfessel, Phys. Rev. A **22**, 2836 (1980).
[15]   J. Harris and S. A. Rice, J. Chem. Phys. **86**, 5731 (1987).

Table 1. Single particle longitudinal and transverse diffusion coefficients in ribbon channels with widths 8, 11, 14 and 20 μm, for several packing fractions.

8 μm channel				
Packing fraction	Stratum	D_{SL} (μm^2/sec)	D_{ST} (μm^2/sec)	D_{ST}/D_{SL}
0.18	1	0.177 ± 0.002	0.105 ± 0.002	0.59
0.18	2	0.187 ± 0.003	0.150 ± 0.003	0.80
0.18	3	0.185 ± 0.003	0.116 ± 0.002	0.63
0.26	1	0.153 ± 0.001	0.078 ± 0.001	0.51
0.26	2	0.161 ± 0.002	0.131 ± 0.001	0.81
0.26	3	0.158 ± 0.001	0.074 ± 0.001	0.47
0.43	1	0.120 ± 0.001	0.056 ± 0.001	0.47
0.43	2	0.123 ± 0.001	0.090 ± 0.001	0.73
0.43	3	0.121 ± 0.001	0.052 ± 0.001	0.43

11 μm channel				
Packing fraction	Stratum	D_{SL} (μm^2/sec)	D_{ST} (μm^2/sec)	D_{ST}/D_{SL}
0.11	1	0.188 ± 0.005	0.122 ± 0.004	0.65
0.11	2	0.202 ± 0.004	0.167 ± 0.004	0.83
0.11	3	0.205 ± 0.004	0.179 ± 0.003	0.87
0.11	4	0.194 ± 0.004	0.142 ± 0.003	0.73
0.40	1	0.122 ± 0.001	0.059 ± 0.001	0.48
0.40	2	0.127 ± 0.001	0.102 ± 0.001	0.80
0.40	3	0.131 ± 0.001	0.110 ± 0.001	0.84
0.40	4	0.129 ± 0.002	0.103 ± 0.001	0.80
0.40	5	0.123 ± 0.001	0.068 ± 0.001	0.55
0.42	1	0.133 ± 0.001	0.072 ± 0.001	0.54
0.42	2	0.130 ± 0.002	0.103 ± 0.002	0.79
0.42	3	0.127 ± 0.002	0.103 ± 0.002	0.81
0.42	4	0.127 ± 0.001	0.101 ± 0.001	0.80
0.42	5	0.126 ± 0.001	0.067 ± 0.001	0.53

14 μm channel				
Packing fraction	Stratum	D_{SL} (μm^2/sec)	D_{ST} (μm^2/sec)	D_{ST}/D_{SL}
0.21	1	0.164 ± 0.002	0.116 ± 0.002	0.71
0.21	2	0.170 ± 0.002	0.149 ± 0.002	0.88
0.21	3	0.170 ± 0.002	0.153 ± 0.002	0.90
0.21	4	0.165 ± 0.002	0.141 ± 0.002	0.85
0.21	5	0.157 ± 0.002	0.101 ± 0.002	0.64
0.25	1	0.160 ± 0.002	0.106 ± 0.001	0.66
0.25	2	0.165 ± 0.002	0.140 ± 0.002	0.85
0.25	3	0.162 ± 0.003	0.139 ± 0.003	0.86
0.25	4	0.164 ± 0.003	0.141 ± 0.002	0.86
0.25	5	0.162 ± 0.002	0.135 ± 0.002	0.83
0.25	6	0.155 ± 0.002	0.097 ± 0.001	0.63
0.44	1	0.113 ± 0.001	0.052 ± 0.001	0.46
0.44	2	0.117 ± 0.001	0.096 ± 0.001	0.82
0.44	3	0.116 ± 0.001	0.102 ± 0.001	0.88
0.44	4	0.120 ± 0.001	0.104 ± 0.001	0.87
0.44	5	0.118 ± 0.001	0.096 ± 0.001	0.81
0.44	6	0.113 ± 0.001	0.054 ± 0.001	0.48

20 μm channel				
Packing fraction	Stratum	D_{SL} (μm^2/sec)	D_{ST} (μm^2/sec)	D_{ST}/D_{SL}
0.17	1	0.150 ± 0.002	0.095 ± 0.002	0.63
0.17	2	0.160 ± 0.002	0.136 ± 0.003	0.85
0.17	3	0.162 ± 0.002	0.146 ± 0.003	0.90
0.17	4	0.163 ± 0.002	0.149 ± 0.002	0.91
0.17	5	0.164 ± 0.004	0.141 ± 0.003	0.86
0.17	6	0.164 ± 0.003	0.143 ± 0.003	0.87
0.17	7	0.164 ± 0.002	0.140 ± 0.003	0.85
0.17	8	0.154 ± 0.003	0.098 ± 0.002	0.64
0.32	1	0.139 ± 0.002	0.081 ± 0.001	0.58
0.32	2	0.155 ± 0.002	0.128 ± 0.001	0.83
0.32	3	0.157 ± 0.002	0.139 ± 0.001	0.89
0.32	4	0.157 ± 0.001	0.143 ± 0.001	0.91
0.32	5	0.151 ± 0.002	0.138 ± 0.001	0.91
0.32	6	0.156 ± 0.002	0.132 ± 0.002	0.85
0.32	7	0.155 ± 0.002	0.130 ± 0.001	0.84
0.32	8	0.148 ± 0.001	0.082 ± 0.001	0.55
0.41	1	0.115 ± 0.001	0.063 ± 0.001	0.55
0.41	2	0.126 ± 0.001	0.102 ± 0.001	0.81
0.41	3	0.130 ± 0.001	0.112 ± 0.001	0.86
0.41	4	0.129 ± 0.001	0.117 ± 0.001	0.91
0.41	5	0.131 ± 0.001	0.119 ± 0.001	0.91
0.41	6	0.131 ± 0.001	0.118 ± 0.001	0.90
0.41	7	0.130 ± 0.001	0.114 ± 0.001	0.88
0.41	8	0.124 ± 0.001	0.105 ± 0.001	0.85
0.41	9	0,120 ± 0.001	0.057 ± 0.001	0.48

Figure Captions

Fig. 1. (Color online) Schematics of a ribbon channel.

Fig. 2. (Color online) Samples of the experimental data for ribbon channels with widths of 5 μm (A), 8 μm (B), 11 μm (C), 14 μm (D), and 20 μm (E), all with packing fraction $\phi \approx 0.4$. The figure shows a superposition of the transverse density profile in the ribbon channel and the single particle diffusion coefficients along and perpendicular to the strata of the transverse density distribution. Error bars are shown; the error per point is typically smaller than the size of the data point displayed.

Fig. 3. (Color online) The single particle diffusion coefficients in the 20 μm channel with packing fraction $\phi \approx 0.41$ along and perpendicular to equal width strata centered on the maxima and minima of the distribution of the transverse density distribution. Note that both the single particle longitudinal and transverse diffusion coefficients are sensibly the same for strata centered on minima and maxima of the density distribution, except for the strata closest to the walls of the channel. Error bars are shown; the error per point is typically smaller than the size of the data point displayed.

Fig. 4. (Color online) (a) Image of 14 μm ribbon channel with packing fraction $\phi \approx 0.44$. (b) Transverse trajectories of the colloid particles in the channel pictured above, as a function of position along the channel. The data were collected over a 5 second interval. Different strata are pictured in different colors (online only), with the density distribution $P(y)$ included as a guide to the eye.

Fig. 5. (Color online) Root mean squared displacement as a function of time in several ribbon channels and the q2D colloid suspension ($\phi \approx 0.27$). The error bars for all data sets, except for q2D, are less than the width of the lines. Error bars for the q2D data set are shown.
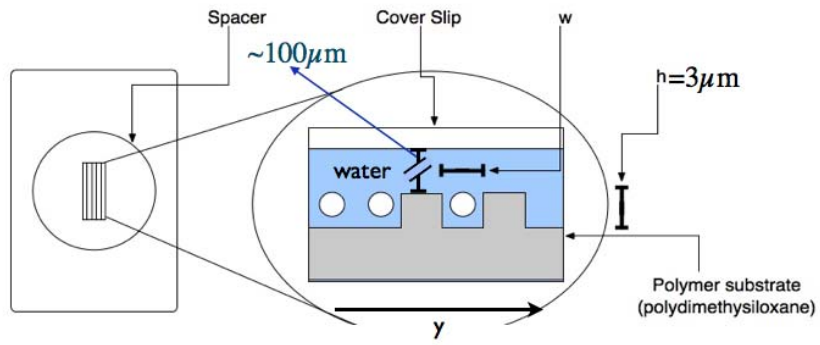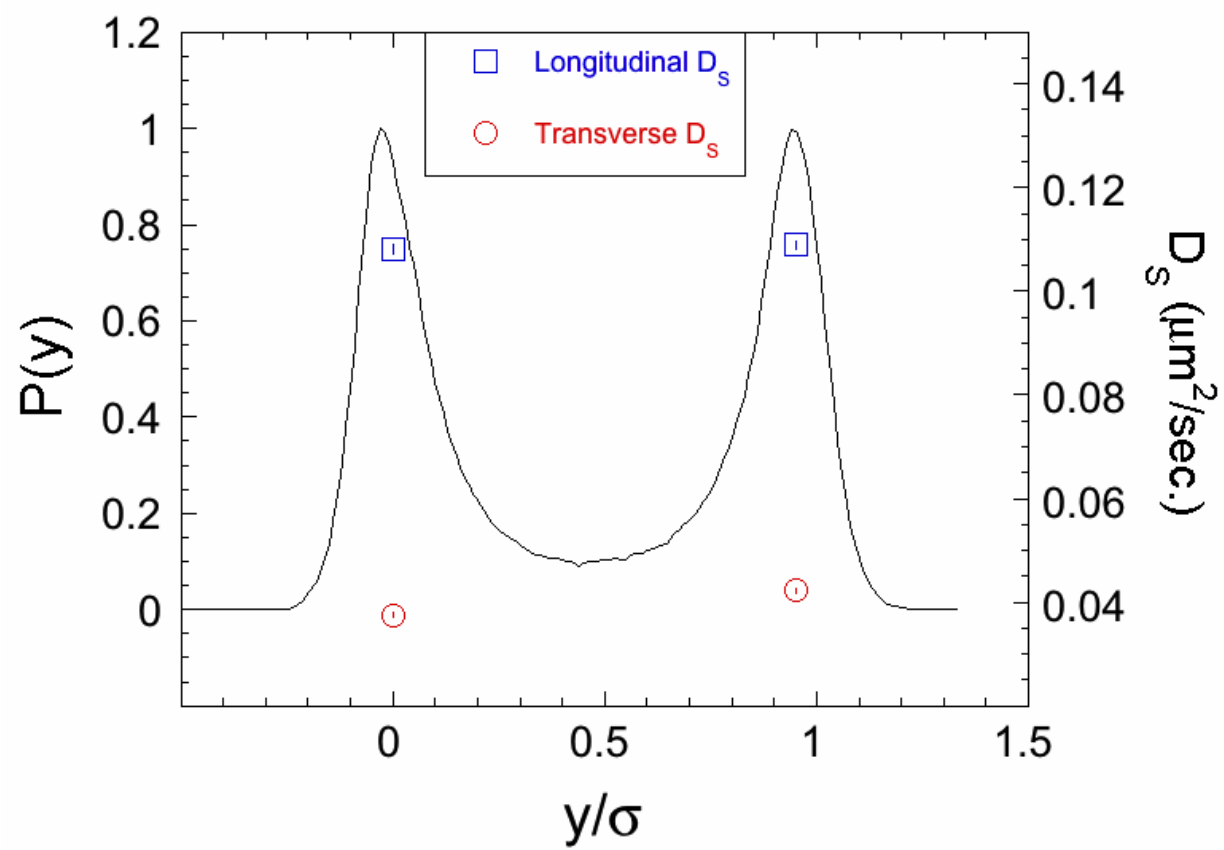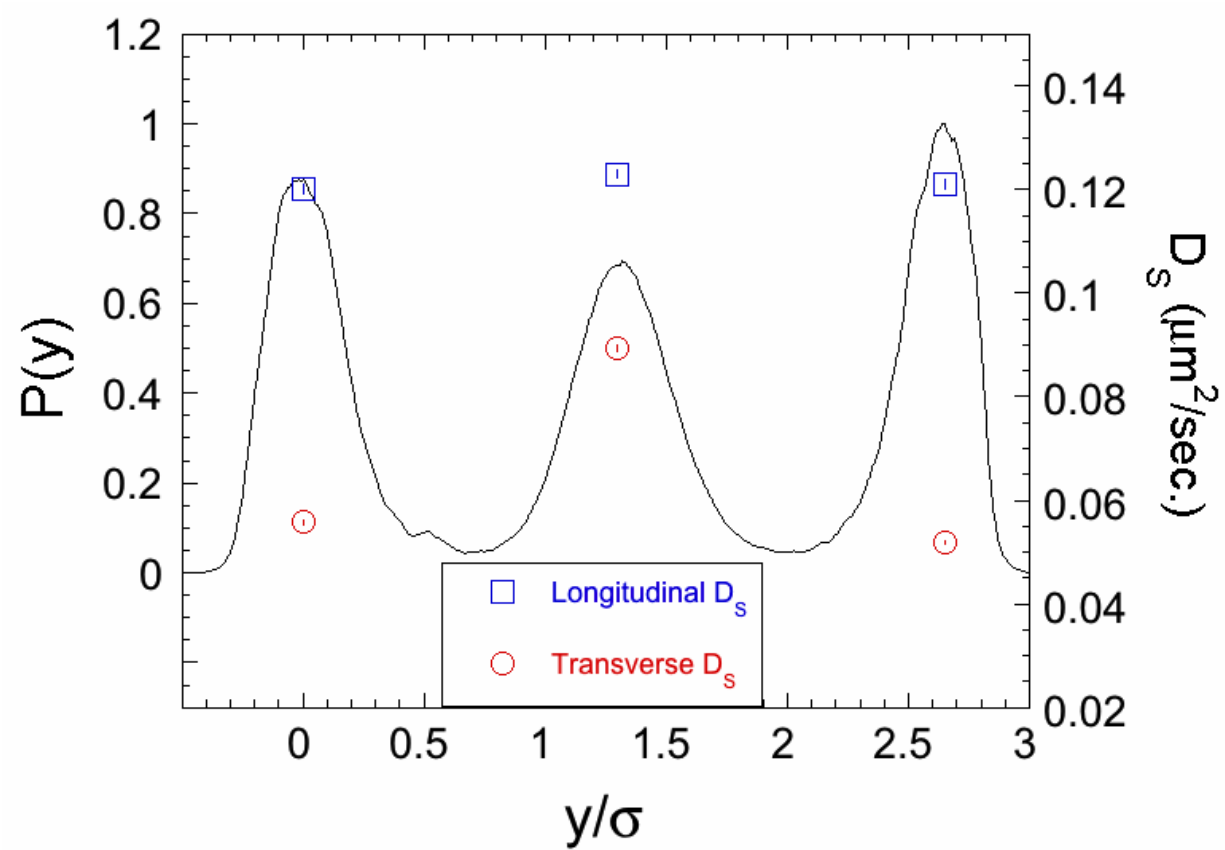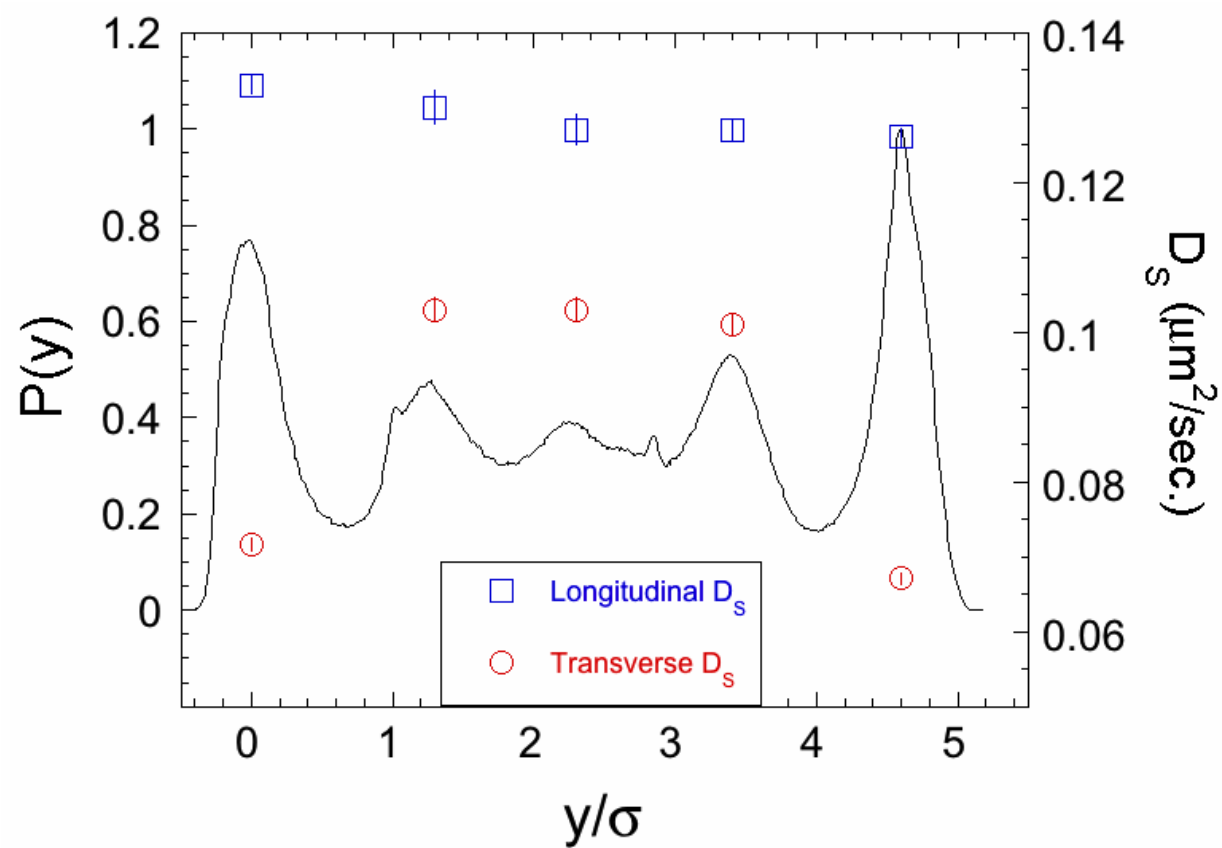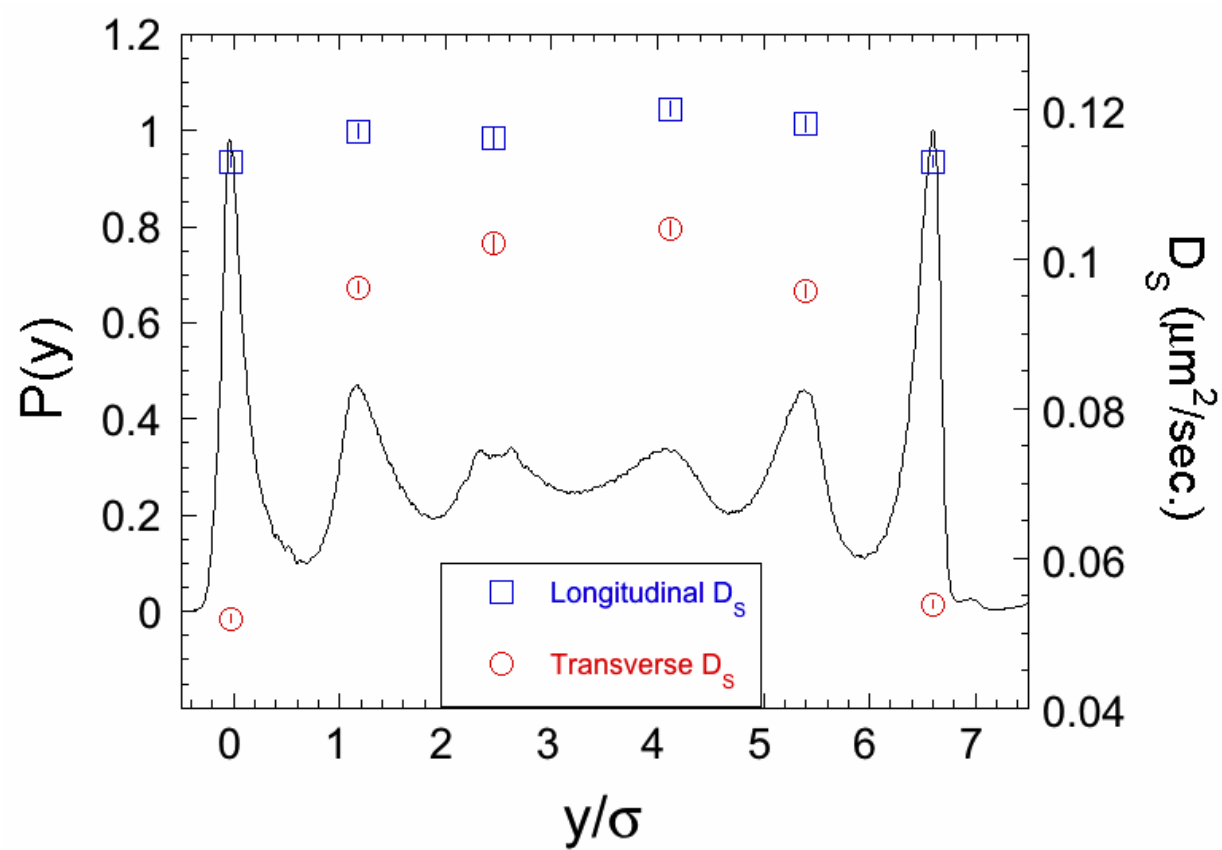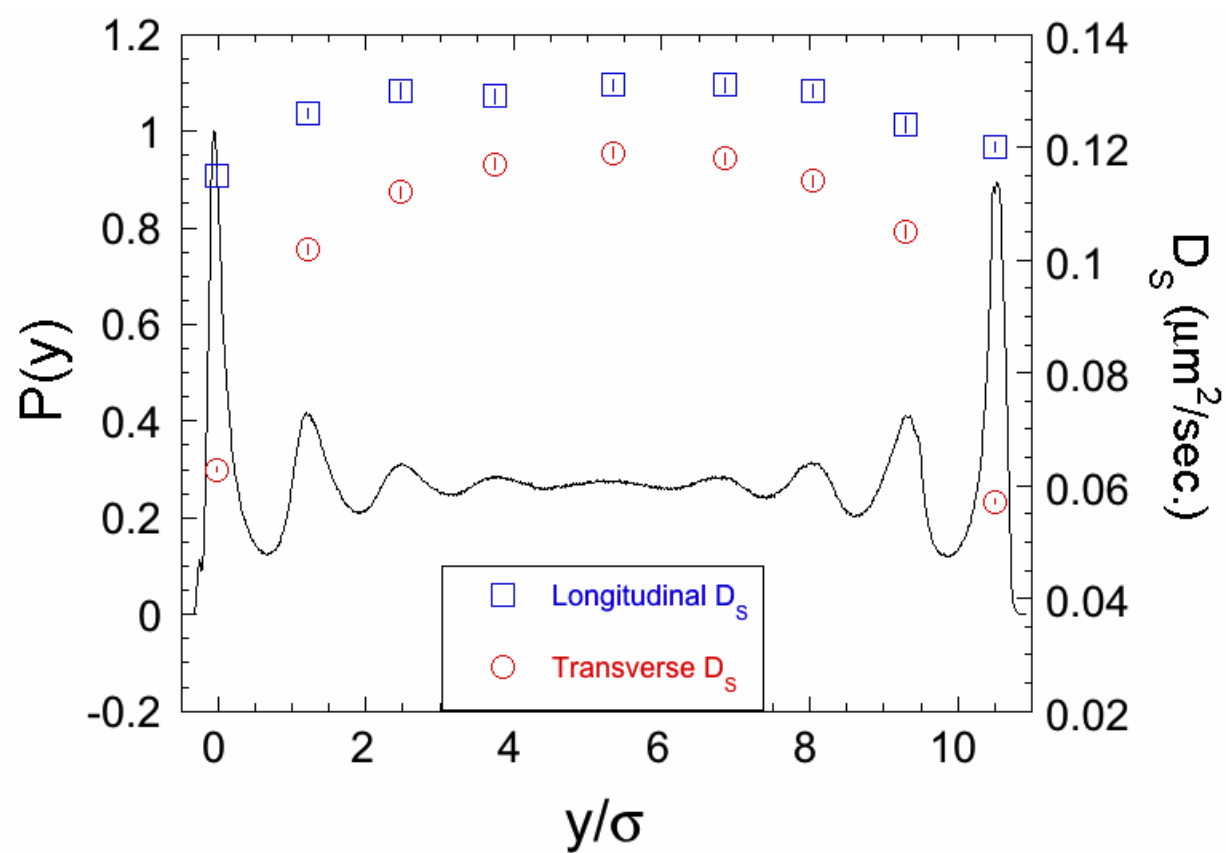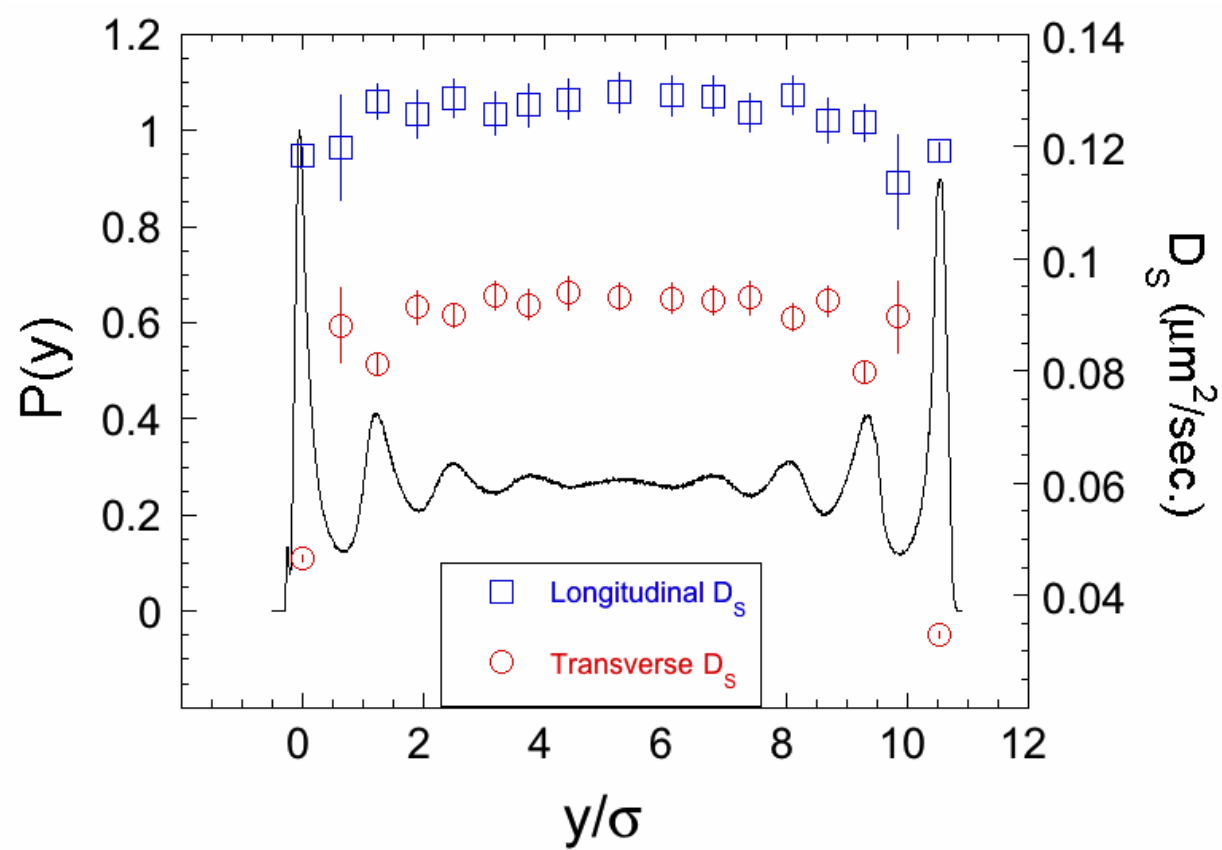
17

Figure 1

Figure 2A

Figure 2B

Figure 2C

Figure 2D

Figure 2E

Figure 3

Figure 4A

Figure 4B

Figure 5